Osseointegration of Hydroxyapatite and Remodeling-Resorption of Tricalciumphosphate Ceramics

MIRIAM DRAENERT,[1*] ALICE DRAENERT,[2*] AND KLAUS DRAENERT[3]
[1]*Clinic for Restorative Dentistry and Periodontology, Ludwig-Maximilian University, Munich, Germany*
[2]*Center of Orthopedic Research, Munich, Germany*
[3]*Zentrum für Orthop Wissenschaften, Munich, Germany*

KEY WORDS tricalciumphosphate; hydroxyapatite; biomaterials; bone remodeling; biodegradability

ABSTRACT *Background:* Cancellous bone defects surrounded by still intact bone structures never heal. Ceramics offer a solution providing osteoconductive scaffolds. *Purpose:* The purpose of the study is to evaluate whether structured β-TCP and HA implants can reconstruct cancellous bone defects, which role micro- and macro-porosity, stiffness and surface area play; finally the indication for both materials based on its resorbability. *Material & Methods:* 10 German Shepard dogs were operated on both tibial heads implanting shell-like fully interconnected ceramic cylinders, using a wet grinding hollow drill coated with diamonds. β-TCP was compared with HA. A polychromatic sequential labelling with 4 different fluorochromes controlled bone formation dynamics. Non-decalcifying histology after perfusion fixation and vessel casting was performed. μ-CT was combined with high resolution microradiography and histology on thin ground crossections. The stages after 6 weeks, 2, 3, 4 months and 15 months were evaluated. *Results:* In spite of osseointegration of HA and β-TCP, the osseointegration of both materials was completely different. Both shell-like bone void fillers were osseointegrated in a sandwich-like manner. HA yielded primarily a reinforcement of the recipient's cancellous-bone bed and full osseointegration after 4 months, whereas β-TCP-implants were fully osseointegrated after 6 weeks. HA did not show signs of resorption. The resorption of the β-TCP resulted during remodelling. The final stage showed restitution "ad integrum" of the β-TCP defects with a physiological architecture, whereas HA was integrated in the cancellous bone construction providing 600 çm measuring macropores showing osteoinductive properties. *Microsc. Res. Tech. 76:370–380, 2013*.

INTRODUCTION

Background

Epi- and metaphyseal cancellous bone defects, which are surrounded by still intact bone structures, never heal (Draenert et al, 1981). The etiology and pathogenesis of bone defects are diverse and frequently involve idiopathic juvenile bone cysts, defects caused by tumors, bone infection, or defects related to open-wedge osteotomies, fractures or loosened artificial components.

Rationale and Objectives

A bone defect, which has been caused by a fracture, is replaced by autologous bone tissue predominantly taken from the iliac crest (Burchardt, 1983; Draenert et al., 2012b; Matti, 1929, 1932, 1936; Müller et al., 1969). In this context, a donor side morbidity of the iliac crest is described, mainly due to pain (Dimitriou et al., 2011; Gerngross et al., 1982; Saxer and Magerl, 1974; Younger et al., 1989). A press-fit inserted ceramic implant can prevent deformation in the donor bed and, consequently, pain (Draenert et al., 2001). In the case of larger defects, tumors or post-traumatic epiphyseal defects or in revisions, one resorts again to the bone bank for homologous grafts involving the risk of infection and tumor transmission (Buck and Malinin, 1994). The main questions are whether structured HA or ß-TCP ceramic implants can yield a physiological reconstruction of a spongeous scaffold, even in large defects, which one of both materials should be preferred and which role play pore size and interconnecting pore width, stiffness, and strength of the material.

Structured calcium phosphate-based bone substitute materials are considered biocompatible and osseointegration can be expected for synthetic ceramics and materials of biological origin as well (Eggli et al., 1988; Tröster, 1993; Wenisch et al., 2003). Bovine sintered ceramics prove to be very stiff and are anisotropic in structure (Draenert et al., 2001). They are sintered at both, high (Tröster, 1993) and low temperatures resulting in different micro-porosities (Donath, 1988; Klinge et al., 1992). Coralliforme HA-ceramics are gathered from corals whose calcium carbonates are transformed

*Miriam Draenert and Alice Draener contributed equaly to this work.
Miriam Draenert, Clinic for Restorative Dentistry and Periodontology, Ludwig-Maximilian University, Munich, Germany

Received 5 November 2012; accepted in revised form 30 December 2012
DOI 10.1002/jemt.22176
Published online 7 February 2013 in Wiley Online Library (wileyonlinelibrary.com).

in the laboratory into HA by a "replaminiforme process" (White et al., 1972, 1986). The question is, whether micro- and macro-porosity or surface area available for colonization by osteoblasts, respectively, stiffness of the ceramic and its influence on bone formation and on bone remodeling are responsible for osseointegration and even osteoinduction (De Long et al., 2007).

The physiological structure of the cancellous bone resembles more the structure of an eggshell, than trabeculae (Draenert et al., 2011; Weidenreich, 1922, 1923, 1930). Shell-formed ceramics, synthetically manufactured with variable interconnections, closely resemble young cancellous bone and, due to their large surface area, are completely overgrown from both sides like a sandwich (Draenert et al., 2011; Wiese, 1998). The indication of the highly nonreabsorbable HA with its higher compressive strength differs significantly from the indication (De Long et al., 2007; Draenert et al., 2011) of the more quickly resorbable β-tricalciumphosphate (TCP) implants (Bohner et al., 2005; Draenert et al., 2011; Eggli et al., 1988). It is an open question, how those embedded resorbable β-TCP ceramics can be reabsorbed (Draenert et al., 2011). Reabsorbable materials are often not stable enough to win the race against time between bone defect healing and resorption and the decomposition of osteoconductive materials. As a consequence, the exact adjustment between material stability and the indication for its use as defect filling material is essential (Bodde et al., 2007; Ng et al., 2008; Tadic and Epple, 2004). The nonreabsorbable HA implants remain bony integrated (Draenert et al., 2011; Holmes, 1979), the morphological processes and differences in bony ingrowth and resorption, and temporary or persistent function, between TCP and HA ceramics remain, for the most part, unexplained. For this reason, this systematic, descriptive study was carried out.

Purpose

The purpose of the study is to answer still open questions whether structured β-TCP and HA implants can reconstruct cancellous bone defects, which role micro- and macro-porosity, stiffness and surface area play for osseointegration. Finally the indication for both materials based on its resorbability and permanent integration, respectively, should be defined.

MATERIAL AND METHODS

Study Design

The cancellous bed of the tibial head in a dog was chosen because it is easily accessible, medially, without incurring large surgical trauma, the main load is carried by the knee's medial compartment, and it is fully vascularized. The operation took place bilaterally to guarantee uniform stress on the rear legs. The animal's growth plates were closed.

Materials

Ten 3- to 5-year-old German Sheppard dogs—eight female and two male weighing between 22 and 35 kg—were operated on. The special set of instruments included adapted drill-guides for the right and left tibial head (Fig. 1a), as well as a set with diamond hollow grinding instruments (Karl Storz Endoscopy) (Fig. 1b) and extractors of sizes corresponding to the implants to be inserted. An adaptor was used for the small ASIF drill (Synthes) to rinse the diamond drills from within.

The synthetically manufactured implants used in this study were of sintered β-TCP (Syntricer® 600) (Fig. 1c) and a HA ceramic (Synthacer® 600) (Karl Storz Endoscopy) (Fig. 1d). Synthacer® and Syntricer® 600 are standardized materials in terms of their complete macro- and micro-porosity and width of interconnections, as well as in size and form. The macropores measure 600 μm in diameter. The cylinder length was between 12 and 19 mm and the diameter of the implants was precisely 8.4 mm over the entire length. The cylinder edges were rounded and one side was closed pore free. The exterior diameter of the diamond drill with which the defect was ground measured 8.35 mm. Consequently the ceramic always had a diameter, which was 5/100 mm larger than the corresponding defect produced by the hollow grinder. The difference in the diameter formed the basis for a stable press fit. The ceramic cylinder was inserted by hand.

Polychromatic Sequential Labeling

To determine the titer dynamics of new bone formation, a polychromatic labeling (Rahn and Perren, 1975) has been performed. Application took place subcutaneously in combination with a local anesthetic. Over a period of a week, oxytetracycline (Pfizer), followed by calcein blue and alizarin, and at last calcein green (Fluka), were given, respectively. The final labeling of the 2- and 3-month stage and after 1 year took place using oxytetracycline, 5 days before the animals were sacrificed with an overdosis Nembutal®.

Operation Procedure

A medial approach to the tibial head was chosen. Access (4 cm) was parallel to the ligamentum patellae. The periosteum was sharply incised through the drill guide 1.5–3 cm below the tibial plateau using the sharp edges of the extractor, which had a diameter of 8.35 mm. The diamond hollow grinder was subsequently positioned. The diamond hollow grinder cut an 8.35 mm measuring bone cylinder using the wet grinding process. The bone cylinder was then broken off at its base and removed from the bed using the extractor. An HA (Synthacer® 600) or a β-TCP implant (Syntricer® 600), respectively, was press-fit inserted. The length of the implant was matched to the length of the removed bone cylinder and was thus as far as possible plane with the facies medialis of the tibia, measuring 12–19 mm. The difference was a result of the distance of the defect to the tibial plateau distally and the width of the medullary cavity at the level of implantation.

Two animals were killed after 6 weeks and two after 2 months, respectively, and three animals after 4 and 15 months. Tissue fixation of all of the animals in this study was performed after sacrificing by perfusion via the abdominal aorta and drainage via the cava vena; the vasculature was casted with MMA. Perfusion, vascular drainage and casting procedure have been previously described (Draenert and Draenert, 1980). The tibiae were dissected and X-rayed on mammography films, the tibial head detached, bloc-stained with alkaline fuchsine, embedded in MMA, and ultimately

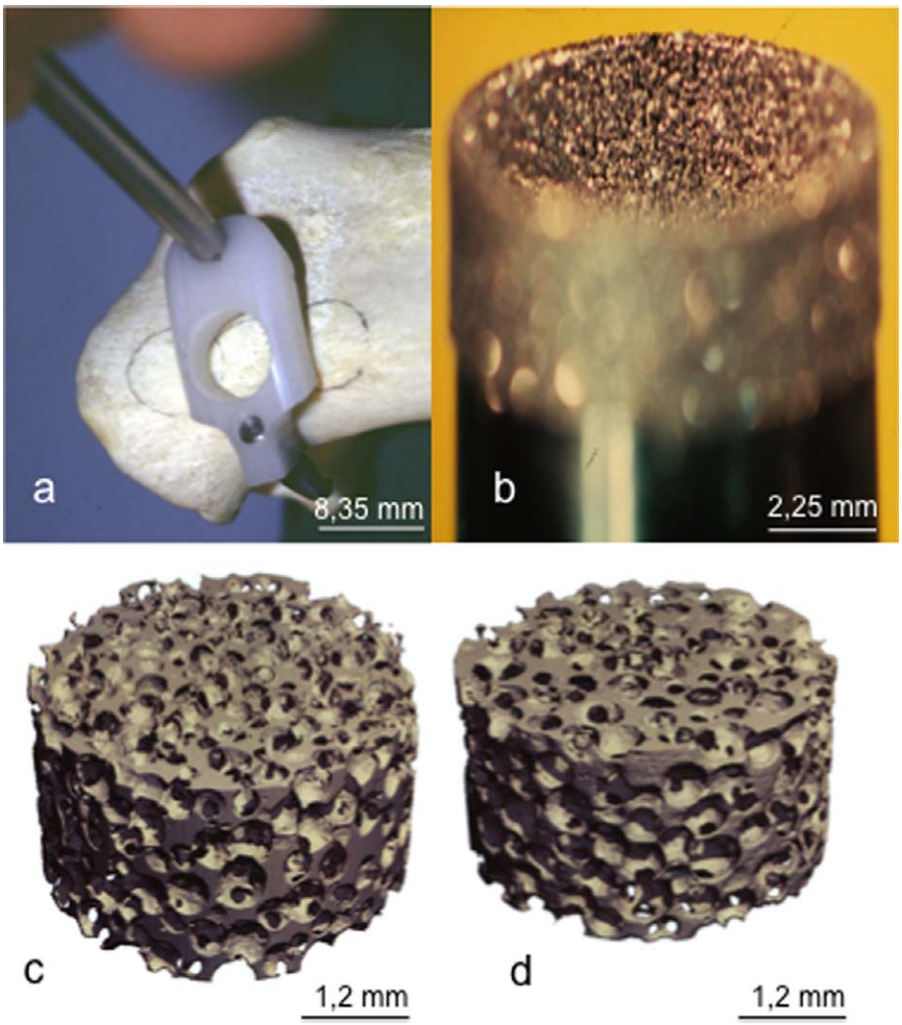

Fig. 1. (**a**) Drill guide on the medial face of the proximal tibia. The diameter of the bone cylinder measures 8.35 mm. (**b**) Grinding instruments coated on both sides and over the rim with natural sharp diamonds. (**c**) Shell-like ß-TCP scaffold presenting a fully interconnected framework of ceramic shells. The 3D reconstruction of μ-CT serial slices in the Scanco® 40 (Zurich, Switzerland). (**d**) Shell-like HA scaffold presenting the same structure with full interconnection (3D reconstruction of μ-CT serial slices).

trimmed to size for the μ-CT. The tissue blocs embedded in methyl methacrylate were CT scanned in a Scanco μ-CT 42 (Scanco, Zurich, Switzerland). The following basic settings were used: high-resolution mode, 300-ms exposure, layer thickness 18 μm, 550–870 slices were recorded per preparation. Initially, the axis of serial sectioning was determined by the long axis of the implant. The blocks were subsequently sliced into 500-μm thick cross sections, ground by hand to a thickness of 110 μm, and then microradiographed at high resolution in the Kristalloflex (Siemens) (Draenert et al., 2012a). The sections were then ground down up to 50 μm and embedded on glasses. Analysis took place in the Leitz (Orthoplan-Ploemopak) using incident fluorescent light, in the transmitted path of light, and in polarized path of rays. High resolution microradiographs and polarized path of rays allowed to differentiate the strain-adapted bone formation adjacent to HA-implants and the different ingrowth depth compared with ß-TCP implants. Documentation was carried out using Ektachrome professional 64 (5400 Kelvin) for the fluorescence and Ektachrome professional 64 T (3500 Kelvin) for the transmitted light images and microradiographs. Three independent scientists analyzed X-rays and histologies. Resorption was judged based on the μ-CT slices and high-resolution histology; pore sizes and interconnections were measured under the microscope and described. The approach of morphometry with μ-CT slices was still not reliable (Draenert et al., 2012a). Strength and stiffness were measured in an earlier study, the ingrowth and different macro-porosities as well (Draenert et al., 2011; Wiese, 1998].

RESULTS

There were no postoperative complications. The animals were able to apply full load on both extremities already on the first postoperative day.

Reconstruction of the Spongeous Scaffold

After 6 weeks, the X rays showed completely healed β-TCP implants revealing a whiteout, merging the

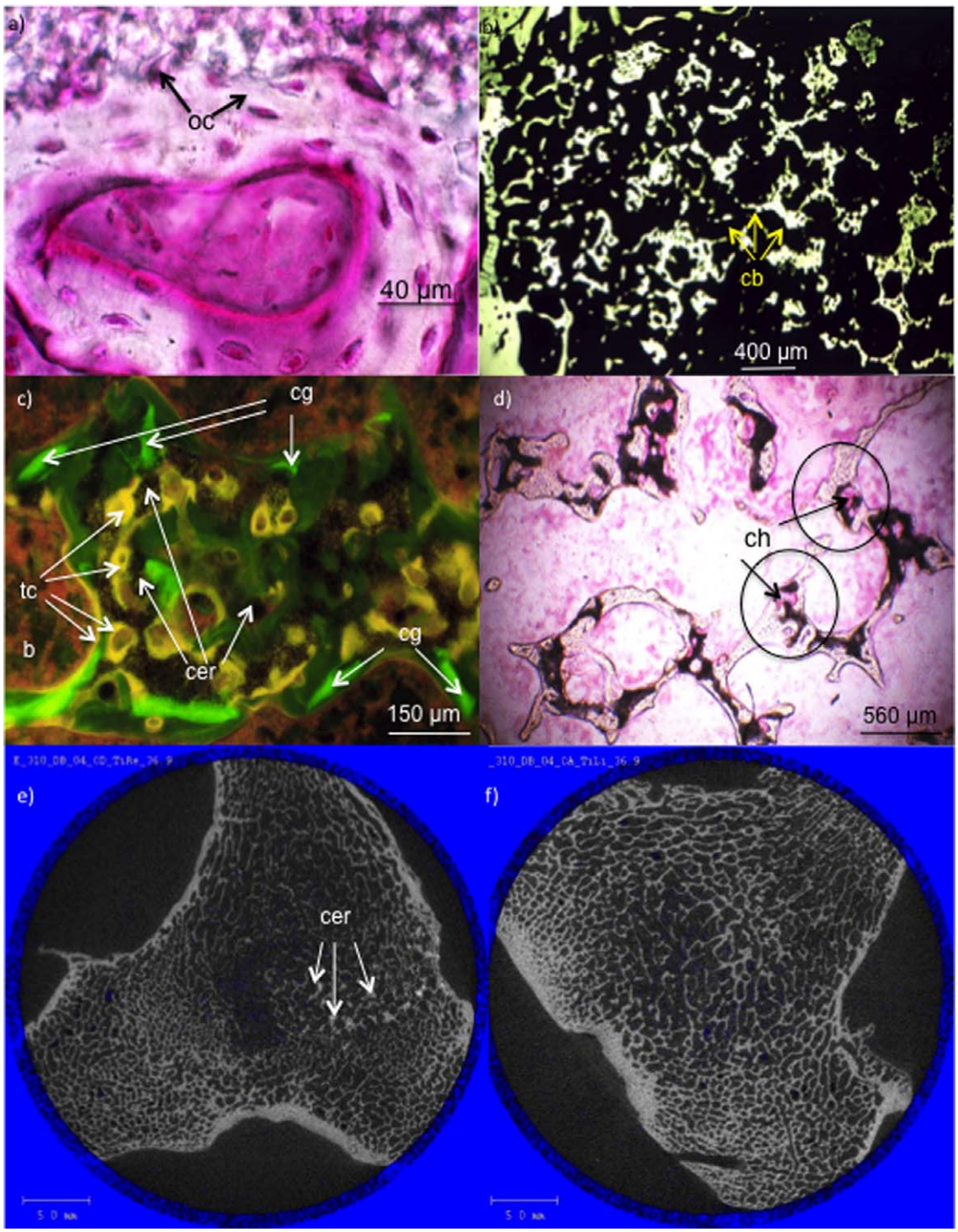

Fig. 2. (**a**) Osseointegration of the β-TCP implant, 6 weeks following implantation, revealing a lamellar arrangement of all osteocytes (oc) thus forming an osteon adhering tangentially to the ceramic surface (**c**). Alkaline fuchsine stained, 40-µm-thin section. Orthoplan Leitz. Oil immersion. (**b**) Similarity of the histological image of the ceramic-bone-gnarls (cb) with the cartilage-bone-gnarls of the growth plate is noticeable. The remodeling-resorption is full in swing. 6-weeks stage. High-resolution microradiograph of the 110-µm thick cross section; Kristalloflex Siemens; Leitz Orthoplan. Ektachr prof. 64T. (**c**) Bone-ceramic-bone gnarl presenting a high turnover rate indicated by the polychromatic labeling, 4 months following surgery. The calcein-green (cg) label from the forth week is still visible with some residues; the ceramic in the center is for the most part reabsorbed (cer); the resorption is followed by new bone apposition labeled with tetracycline of the last week before sacrificing (tc). Incident fluorescent light with FITC filter in the Leitz Orthoplan, Ploemopak. Apochromat ×10, oil. Ektachrome prof 64 5400 Kelvin. (**d**) The delicate cancellous bone scaffold reveals sandwich-like embedded residues of the β-TCP ceramic, 4 months after implantation. The remodeling-resorption process, revealing cutter heads (ch, circle) is still in progress. Alkaline fuchsine stained, 40 µm-thin cross section. Orthoplan, Leitz. Ektachrome prof. 64T. (**e**) The remodeling-resorption of the β-TCP implant is nearly finished after 4 months. There are minor residues of TCP embedded in the newly formed bone (cer). µ-CT slice, Scanco 40. (**f**) The β-TCP cylinder has been reabsorbed and the physiological scaffold is reconstructed revealing a restitution ad integrum. µ-CT slice, Scanco 40.

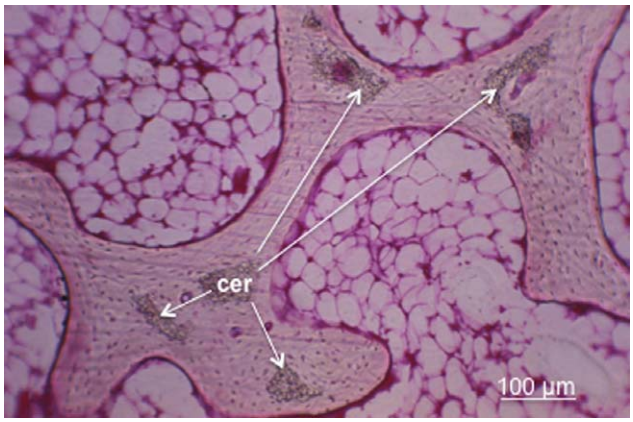

Fig. 3. The physiological framework of cancellous bone reveals minor residues of the ceramic (cer), completely embedded in the bone; the bone marrow has returned to normal fat marrow. Alkaline fuchsine stained, 30-µm-thin cross section. Orthoplan, Leitz. Ektachrome prof. 64T.

contrast into the bone contrast. They were bony integrated and the ceramic surface was tangentially completely overgrown (Fig. 2a). In accordance with cartilage-bone-gnarls of the growth plate, the similarity of the histological image as ceramic-bone-gnarls was noticeable (Fig. 2b). The labeling reveals a pronounced turnover (Fig. 2c). The graceful cancellous bone framework still partially surrounds ceramic residues (Fig. 2d). After 4 months, the cancellous bone architecture was almost entirely reconstructed (Fig. 2e). In contrast to the HA-implant at 15 months, the cancellous bone of the TCP implants' tibial head reveals restitution "ad integrum" (Fig. 2f). In single cases, trabeculae containing ceramic residues are found embedded as ceramic-reinforced bone (Fig. 3). In spite of the same pore sizes, there was a pronounced difference of the bony ingrowth of the two materials.

The HA-implants showed after 6 weeks a whiteout as well and osseointegration along the interface. The bony ingrowth had not advanced to a depth of more than two pores into the implant. There was a tangential adherence of the newly formed bone on the shell-like ceramic surface (Fig. 4a). Following a period of 2 months, osseointegration had further advanced. The high-resolution microradiograph showed that ordered lamellar bone structures had grown through the pores of the implant and that the ceramic had integrated as a building block in the total construction of the cancellous framework. The ceramic scaffold was free of microfractures in both materials and all small pores were overgrown with mature, vital bone (Fig. 4b). After 4 months, the HA implant was part of a harmonious ceramic-bone-construction, newly formed lamellar bone, on the medial as well as along the dorsal cortical bone, supported the ceramic cylinders (Figs. 4c and 4d). Mature, closely layered lamellar bone pervaded by arterial vessels covered the bordering pores and supported the bone in the implant (Fig. 4e). Following 15 months, a high-resolution microradiograph showed that the construction of HA-ceramic and newly formed bone is complete: there are no visible fractures in the ceramic scaffold. The HA implant is supported by over the entire surface and integrated into the bone structure. The most varied lamellar bone formations are to be seen in the interior of the pores: ring-shaped linings contrast to spike constructions and complete compactions are found. Domed and support constructions are seen in the interface between implant and bed. Ceramic and newly formed bones build an overall construction (Fig. 4f).

The interconnections measured 100–150 µm and allowed the fast ingrowth of newly formed vessels comprising concentric lamellae of newly formed bone. The macropores allowed the formation of complete Haversian systems. The fast colonization in the β-TCP implants yielding osseointegration was complete after 6 weeks, in one animal after 2 months, whereas HA-implants showed complete osseointegration in the 4-month stage (Fig. 5).

The Role of Surface Area, Implant's Stiffness and Bone Response

After 6 weeks, both implants had been bony integrated and the ceramic surface of both was overgrown tangentially. Noteworthy in the µ-CT was, that the bone response along the interface and the bony support of the HA implants were stronger compared with the β-TCP implants. On the other side, the bony ingrowth and resorption with the β-TCP implants had advanced compared with the HA implants and toward the center. The X-ray contrast of the HA implant had increased after 2 and 4 months, while that of the β-TCP implant had been nearly completely disappeared (Figs. 6a and 6b). The reinforcement of the adjacent spongeous bone in HA implants revealed a lamellar concentric apposition of newly formed bone along the whole interface. The lamellar concentric reinforcement of the bed was lacking in the TCP implants. In later stages, the strengthening of the adjacent cancellous bone in the HA implant site was even more defined; partly the cancellous bone was converted to a compact one.

Resorption of ß-TCP Versus HA: Strength and Osseointegration

Resorption of the β-TCP implant was already advanced at the 6-weeks stage, the X-ray contrast blurred and partially indistinguishable from the bone, only residues of the ceramic scaffold were recognizable. Fifteen months following surgery, the HA implant appeared as a nearly solid implant, while the β-TCP implant was, in one animal, totally and in two animals, nearly completely reabsorbed (Figs. 6c and 6d). The β-TCP resorption varied slightly from animal to animal. Whereas osteoclasts were barely visible in the HA implants at this stage in and on the implants, the cutter heads, comprised of multinucleate giant cells followed by osteoblast layers on the ceramic and bone, were found on the histological image of the TCP implants (Fig. 7). There were no differences in the histological findings for either animal at this stage except the mentioned slight difference in resorption in β-TCP implants.

Even in HA-implants rarely cutter heads were found. There was no striking difference of the findings in the 3-months stage. Compared with the HA, the TCP implants were nearly completely reabsorbed and higher resolution on thin sections showed, however,

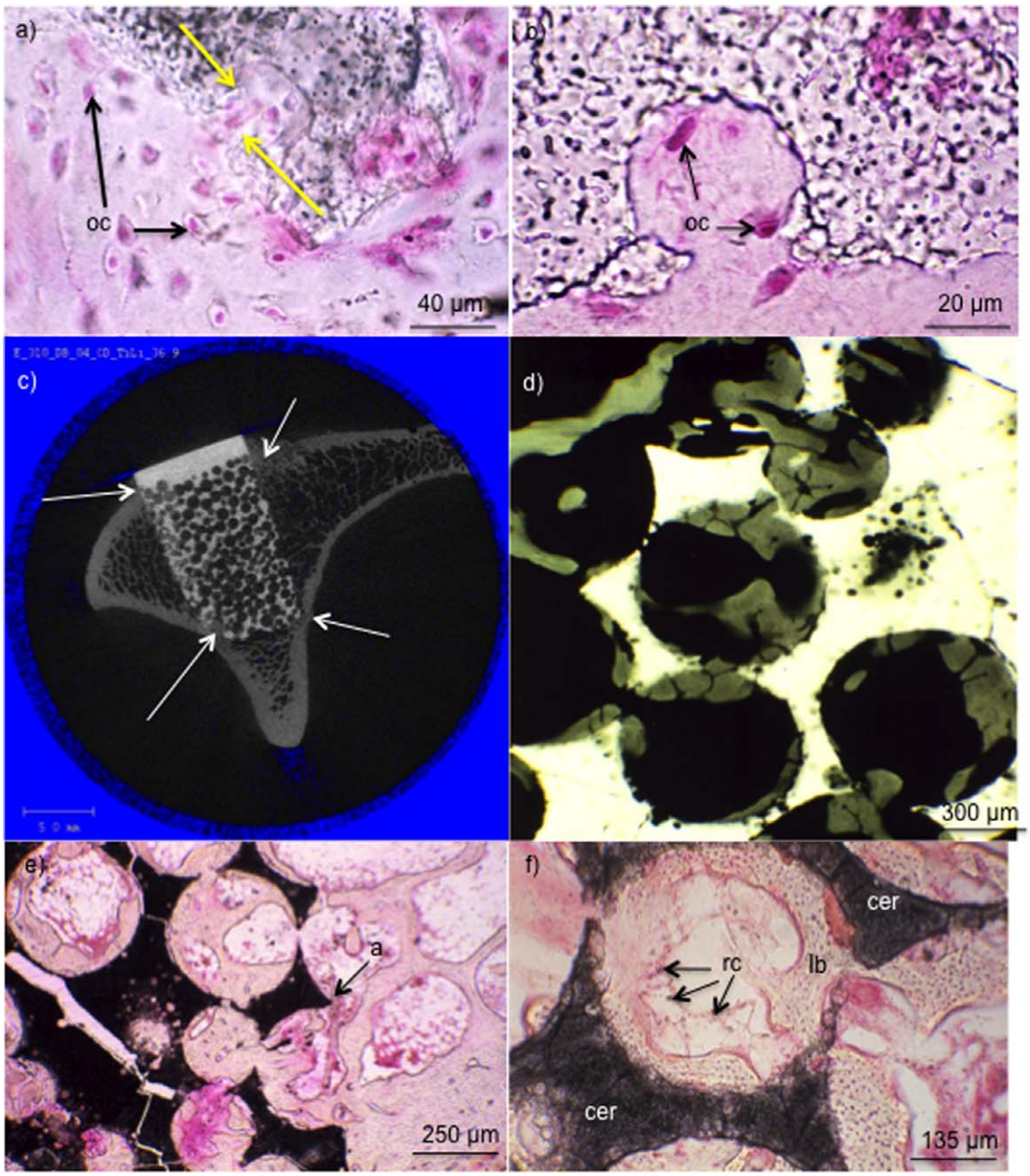

Fig. 4. (**a**) Osseointegration of the HA-implant, 6 weeks following implantation, revealing fully mineralized woven bone with irregular arrangement of osteocytes (oc), filling even ceramic pores measuring <20 µm in diameter (arrow). Alkaline fuchsine stained, 30-µm-thin section. Orthoplan Leitz. Oil immersion. Kodak Ektachrome prof. 64T. (**b**) 40-µm-measuring micro pore filled with fully mineralized bone, revealing osteocytes (oc) within their lacunar-canalicular system; 2-months stage of the HA implant. Alkaline fuchsine stained, 30-µm-thin section. Orthoplan Leitz. Oil immersion. Ektachrome prof. 64T. (**c**) 4 months following implantation the HA-implant reveals compact bone near the cortical bone and in the outer pores of the ceramic. There is a strong bony support from all cortices (arrows). µ-CT slice, Scanco 40. (**d**) Osseointegration of the HA implant as part of the construction of the lamellar spongeous-bone scaffold; 4 months following the implantation. High-resolution microradiograph of the 100-µm thick cross section; Kristalloflex Siemens; Leitz Orthoplan. Ektachr prof. 64T. (**e**) 4 months following implantation, the HA implant has become part of the bone construction; mature and fully mineralized lamellar bone forms a ceramic-reinforced bone scaffold. The straight path of the artery (a) is revealed due to the casting of the vasculature. Alkaline fuchsine stained, 40-µm-thin cross section. Orthoplan, Leitz. Oil immersion. Ektachrome prof. 64T. (**f**) HA-ceramic implant (cer), 15 months following surgery. Sandwich-like ceramic-reinforced cancellous bone revealing fully mineralized lamellar bone (lb) and a normal bone marrow with phagocytized ceramic particles within reticulum cells (rc). Alkaline fuchsine stained, 40-µm-thin cross section. Orthoplan, Leitz. Ektachrome prof. 64T.

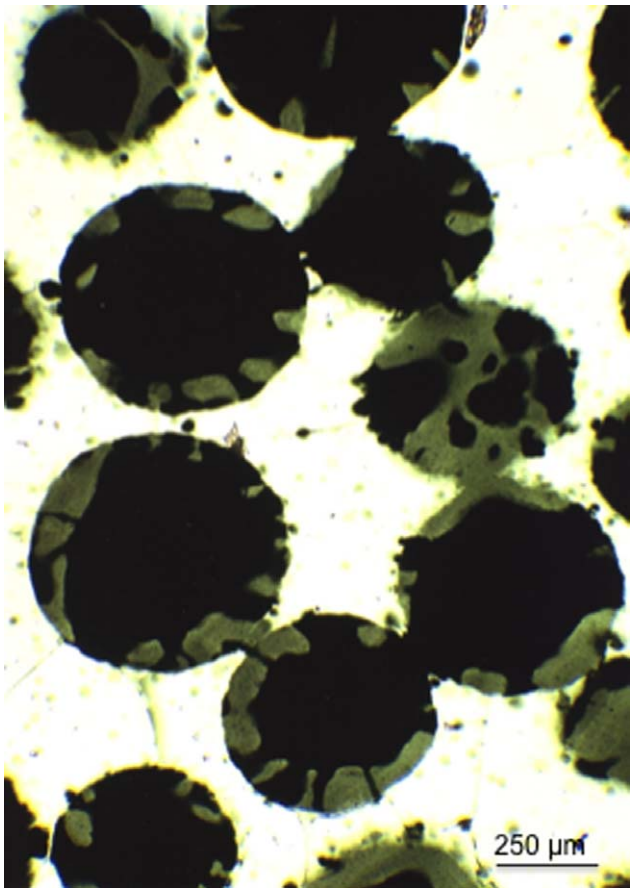

Fig. 5. Ceramic reinforced bone construction, 15 months after implantation of an HA ceramic. In the center of the implant still mature lamellar bone is presented. A structured architecture is revealed. High-resolution microradiograph of the 100-µm thick cross section; Kristalloflex Siemens; Leitz Orthoplan. Ektachrome prof. 64T.

that remodeling-resorption on the bone and ceramic was advancing.

Even if resorption is barely detectable in general, high-resolution images show several cutter heads on the HA-implant and along the interface. Intracellular ceramic crystals are seen in the reticulum cells of the bone marrow.

DISCUSSION

Bone Grafts

Skeletal trauma surgery requires bone and osteochondral grafts for timely reconstructing musculoskeletal injuries; the sources for autologous grafts are limited and application of bank bone might be conflicting, therefore the use of ceramic bone substitutes, plain or combined with growth factors present the preferential treatment, at least as osteoconductive materials, where a defined compressive strength of the material is considered sufficient for defect healing (De Long et al., 2007; Draenert et al., 2011).

The purpose of the study was to clarify whether ceramic bone void fillers yield a reconstruction of cancellous bone defects, to work out differences of both materials HA and β-TCP based on stiffness and strength and surface area, to answer the question of optimal pore-size and to define the final outcome after resorption and permanent osseointegration, respectively.

Limitations of the Study

As a descriptive study, the evidence of the investigation is limited due to the lack of quantification by morphometry, the number of animals per stage, which did not allow a statistical analysis. Even morphometry of series of µ-CT slices were considered limited due to a restricted resolution of in-bone embedded ceramic material. Nevertheless, the high-resolution histology allows to understand the complicated processes, how cancellous bone defects are reconstructed, Haversian systems form within pores providing a defined diameter, how sandwich-like embedded ceramics can be reabsorbed during remodeling and ceramic-reinforced bone constructions are built.

Ceramic Bone Substitutes and Reconstruction of the Cancellous Scaffold

The Ca-phosphate crystals have a close relationship to the periodic banding of type I collagen (Robinson and Watson, 1952, 1955). The tangential colonization through the osteoblasts is closely connected to the specific surface of calcium-phosphate scaffolds (Draenert et al., 2011). The HA and β-TCP implants in this study do not vary in their biocompatibility from the materials in other studies (De Long et al., 2007; Draenert et al., 2011; Eggli et al., 1988; Ferraro, 1979; Fujita et al., 2003; Jarcho et al., 1977; Moore et al., 1987; Schieker et al., 2008; Winter et al., 1981).

Differences of HA and ß-TCP Integration

The HA implants in this study with a macroporosity of 600 µm were all bony integrated up to the second row of pores after 6 weeks and they were fully integrated into the bony scaffold after 4 months.

The image of osseointegration with β-TCP implants was different. In the evaluation of the histology, the β-TCP implants were completely grown through after 6 weeks and later stages accentuated the complex process of remodeling-resorption. The sandwich-form bony embedding was similar in β-TCP implants with similar macrostructures. The process, however, was substantially more rapid. The explanation can be seen in the lesser degree of stiffness and the omission of the stress shielding effect. Both materials yield a reconstruction of the scaffold, β-TCP resembled a physiological cancellous bone, whereas HA presented a new material: ceramic reinforced bone.

The Role of Pore Size, Stiffness, and Surface Area

As far as the physical characteristics are concerned, solubility in a physiological environment on the one hand (De Groot, 1980; Gmelin, 1957; Jarcho, 1981), and stiffness and compression strength on the other hand (Draenert et al., 2011) are of importance for osseointegration. HA is practically insoluble in a physiological environment while β-TCP reveals rapid liquid absorption and pronounced solubility (De Groot, 1980; Gmelin, 1957; Jarcho, 1981). This explains the rapid decline in stiffness, no stress protection, but also no osteoinduction and its biodegradability. Because of its

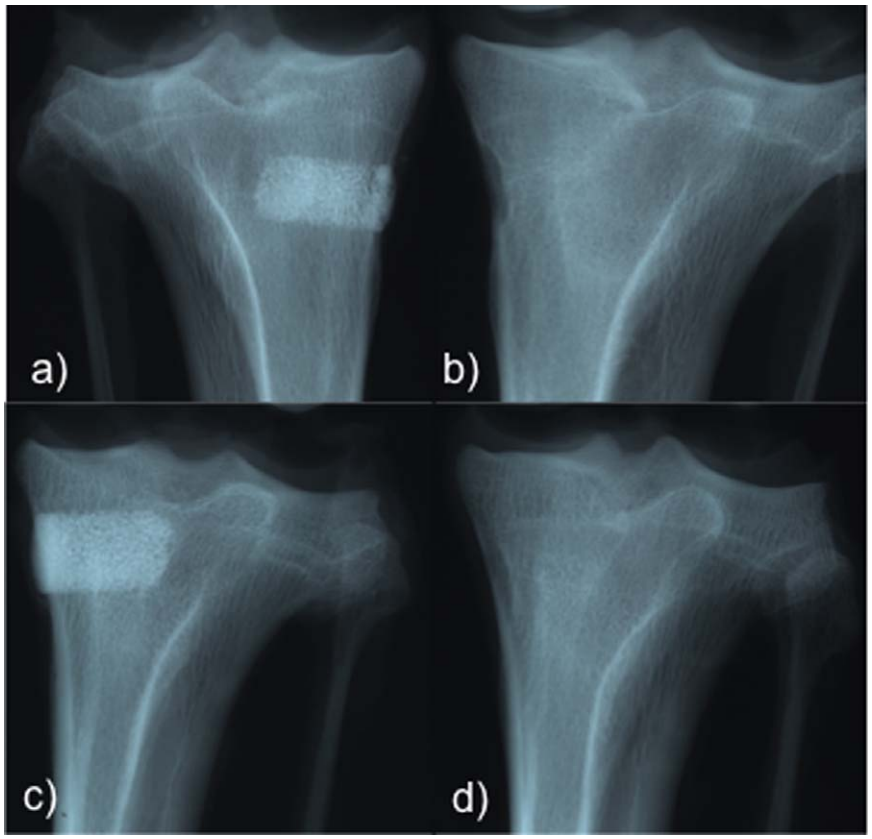

Fig. 6. (**a**) Contrast enhancement of the HA implant. 4 months following surgery. Anterior-posterior (ap) X-ray on Kodak high-resolution film. (**b**) Nearly complete reabsorption of the β-TCP cylinder in the tibial head. 4 months after implantation; ap X-ray on Kodak high-resolution film. (**c**) Pronounced contrast of the HA cylinder after 15 months; ap X-ray on Kodak high-resolution film. (**d**) Restitutio ad integrum of the tibia after β-TCP implantation, 15 months following implantation.

damping properties, β-TCP could be successfully combined with HA (Draenert et al., 2012a).

Bone ingrowth is interpreted in very different ways in the numerous studies using animals and is related in every case to macroporosity. Klawitter and Hulbert (1971), Klawitter et al. (1976), Nade et al. (1953) and Kühne et al. (1994) all base their studies on a pore size of 100 μm, a size under which no bony ingrowth should occur. The discussion is not a new one and has already been conducted in the field of prosthetics (Bobyn et al., 1980). With respect to this study's findings, which demonstrate that micropores and fissures having a diameter smaller than 5 μm showed bony ingrowth, this question must be considered unanswered. As a consequence, the complex biomechanical situation of strain-adapted bone remodeling must be taken into particular account. Tibial head and the distal, medial femoral epiphysis are highly stressed bone sections, a fact, which is revealed in their dense cancellous bone structure (Wolff, 1870). Such a bed allows for aggressive bony ingrowth even in small and the smallest of pores (Eggli et al., 1988).

The Role of Surface Area

The ingrowth rates of shell-form ceramic implants, presenting a large shell-like surface area available for colonization, were significantly higher than reported for the ingrowth of bovine materials: a 5.4mm in diameter measuring cylindrical implant of a shell-like synthetic HA was osseointegrated after 23 days, whereas the same cylinder of bovine material revealed bony ingrowth only after 2 years once the microfractures resulting from fatigue stresses had reduced stiffness

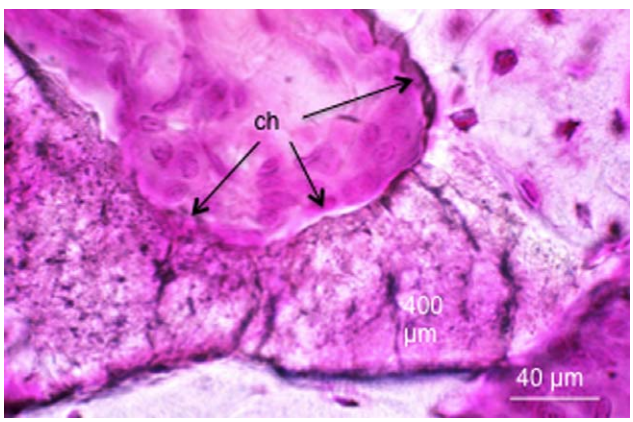

Fig. 7. Cutter head (ch) of osteoclasts penetrating the β-TCP ceramic and bone (arrows). The ceramic is fully osseointegrated. Alkaline fuchsine stained, 40-μm-thin cross section. Orthoplan Leitz. Oil immersion.

(Draenert et al., 2001; Wiese, 1998). Compared with the β-TCP implants in this study, colonization of the HA surfaces was slower. There are also differences with respect to incomplete osseointegration to materials of biological origin, which are structurally anisotropic and bony ingrowth is sometimes hindered for structural reasons (Draenert et al., 2001), while the implants presented here, are structurally isotropic, meaning they are in essence equally strong in all directions. Neither the coral forms nor the bovine materials meet this requirement (Holmes et al., 1984; Tröster, 1993; White and Shors, 1986).

Osteoinduction and Remodeling of Stiff Implants

The low level of solubility and pronounced stiffness of HA implants causes a larger deformation at the implantation bed, resulting in an osteoinductive and remodeling effect. Stiff implants such as bovine hydroxyapatite or more pronounced aluminum oxide implants could demonstrate two phenomena: relative movement at the interface and stress shielding; both could lead finally to the formation of fibrous tissue (Klawitter and Hulbert, 1971; Uchida et al., 1984). A stiff implant transmits introduced energy further, subsequently is there no bone formation within the pores of a stiff implant (Draenert et al., 2012a). This bone response can be interpreted as a mechano-induction or protection, respectively (De Long et al., 2007; Draenert et al., 2001, 2011) and is clearly visible in the HA-implants of this study.

Resorption of ß-TCP and the HA-Bone Construct

Calcium phosphate ceramics are broken down in two distinct ways as a result of chemical–physical solubility and disintegration of the granules subsequently broken down by phagocytosis initiated by macrophages or via foreign body giant cells, osteoclasts or ceramoclasts (Meiss, 1986). Such multinucleated giant cells were found on the β-TCP material as well as on the HA material in this study, as in other studies (Eggli et al., 1988; Meiss, 1986). The chemico-physical solubility is certain to play a role especially in the disintegration of the crystallites in β-TCP. It is practically not existent in HA (Eggli et al., 1988; Gmelin, 1957). The literature reports β-TCP implant resorption rates of up to 85% after 6 months (Cameron et al., 1977; Eggli et al., 1988; Ferraro, 1979; Klein et al., 1983; Koerten and van der Meulen, 1999; Levin et al., 1974; Peelen et al., 1979; Renooij et al., 1985; Shimazaki and Mooney, 1985; Wenisch et al., 2003; Yamada et al., 1997). It is assumed that the large-pore β-TCP ceramics are absorbed at a somewhat slower rate as they are not as quickly ingrown with tissue (Eggli et al., 1988). This would not explain the differences in our study because all implants reveal equally large macropores. De Groot (1980) stated that microporosity was responsible for resorption. The close connection between remodeling and resorption was particularly striking in this series. The apparent result of remodeling-resorption was ceramic-bone-gnarls in analogy to the cartilage-bone-gnarls in the remodeling of the growth plate (Weidenreich, 1930). In the final stage, 14 months after implantation, only small amounts of residues, such as interstitial lamellae, were occasionally found in the otherwise physiologically formed bone trabeculae whose architecture was no longer distinguishable from the surroundings. This remodeling-resorption phenomenon also easily explains the difference between increased resorption activities in small-pore β-TCP implants as opposed to the large-pore implants in the study conducted by Eggli et al. (1988). Remodeling activities must unavoidably occur on a larger scale in small-pore, denser implants if physiological cancellous bone is ultimately to be restored.

The HA-Bone Construct

According to the findings of this study, pore size plays a role especially in the integration of ceramic implants in the overall construction of the cancellous framework. Wiese (1998) was able to show that shell-form HA ceramics in the epiphysis with 300-μm-large pores had integrated so completely in the physiological architecture that the implants were hardly recognizable, whereas a diameter of 600 μm adapted better in the metaphysis. This study's findings show harmonious integration of the 600-μm-large macro-porous ceramics in the cancellous bone of the tibial head. These size data result from Haversian system measurements, which normally have a diameter of between 50 and 100 μm, and the sizes of epiphyseal and metaphyseal cancellous bone honeycombs, with diameters of 300 and 400 μm and 600 and 800 μm, respectively.

It is generally assumed that hydroxyapatite is hardly resorbable. This fact ultimately even ended up in the Guidance for Industry and FDA Staff (2003) (Holmes et al., 1984; Hoogendoorn et al., 1984; Klein et al., 1983; Renooji et al., 1985). Holmes et al. (1979) were the first to see resorption activities in hydroxyapatite as dependent from stress and strain. Their mandibular model (Holmes et al., 1979) recorded "substantial" biodegradation within a period of 12 months, whereas the model with a cortical window in the radius (Holmes et al., 1984) and a small load exhibited only little substance loss over a period of 12 months. Jarcho (1981) had already proven the considerable difference between β-TCP and HA. There is little evidence that miniscule differences in the manufacturing processes or even impurities of HA (Eggli et al., 1988; Hoogendoorn et al., 1984; Schilling et al., 2004; Shimazaki and Mooney, 1985; Yamada et al., 1997) are responsible for the varying findings in reference to HA resorption. It is more probable that calcium carbonate and calcium-phosphate residues are responsible for resorption rates of over 20% in the first months (Holmes et al., 1984). Findings with signs of resorption on pure HA implants had one thing in common: the cutter heads were narrow and the lacunae among the giant cells were small and flat compared with the Howship' lacunae in bone or in ß-TCP. These phenomena are thus easy to explain in that HA represents the more stable chemical substrate, which in turn is less readily resorbed (Gmelin, 1957).

Bone-HA Construct

In the final analysis of HA-implants, a new material emerges: ceramic reinforced bone (Draenert et al., 2001; Holmes et al., 1984). The breakdown of calcium

phosphate in the body is dependent on the emission of protons from the bone-resorbing cells in the direct surroundings, this means via the osteoclasts or the "ceramoclasts," respectively (Meiss, 1986). The morphological correlate to the resorption fronts is represented by the suction cups of the osteoclasts with the ruffled borders visible in electron microscopic images (Dudley and Spiro, 1961; Schenk, 1974; Scott and Pease, 1956). The protons make it possible to dissolve hydroxyapatite crystals. The acidic lysosomal enzymes of the osteoclasts digest the organic ground substance of bone, such as collagen. The low power view of those HA-implants reveal a harmonic construct of a bone scaffold combined with HA-supports or reinforcing lamellae (Draenert et al., 2001, 2011; Holmes, 1979; Holmes et al., 1984).

Ceramic Reinforced Bone

It can be assumed that bone sections strengthened with ceramic and showing a greater degree of stiffness could have negative effects on the joint. On the other hand, they could be very beneficial with respect to osteoporosis. The harmonious image of integration with the expansive colonization of the ceramic surfaces, in combination with their high strength of the material, in any case emphasizes the benefits of the shell structure and decreases the significance of further efforts regarding microporosity and the incorporation of silicon or silicates in HA structures, or even biphasic ceramics (Cordell et al., 2009; Urban et al., 2007; Vallet-Regi, 2006).

CONCLUSION

Both materials, HA and β-TCP yield a reconstructed cancellous bone defect, both are osteoconductive. Osseointegration does more depend upon the biomechanical force acting on the implant than from pore sizes; stiff HA-implants clearly show osteoinductive response; β-TCP-implants are faster integrated, fully reabsorbed by a complicated remodeling-reabsorption process; the compressive strength of shell-like implants providing a large surface area for colonization offer enough stability to last for defect healing due to their sandwich-like colonization with newly formed bone. HA-implants yield a new material, ceramic reinforced bone and might therefore be preferred where severe deformation of the bone structure can be expected, such as in donor defects of the iliac crest or supporting the cartilage baseplate of the tibial head or even stiffening the structure of the calcaneus.

REFERENCES

Bobyn JD, Pilliar RM, Cameron HU, Weatherley GC. 1980. The optimum pore size for the fixation of porous-surfaced metal implants by the ingrowth of bone. Clin Orthop Relat Res 150:263–270.

Bodde EW, Wolke JG, Kowalski RS, Jansen JA. 2007. Bone regeneration of porous beta-tricalcium phosphate (conduit tcp) and of biphasic calcium phosphate ceramic (biosel) in trabecular defects in sheep. J Biomed Mater Res A 82:711–722.

Bohner M, van Lenthe GH, Grünenfelder S, Hirsiger W, Evison R, Müller R. 2005. Synthesis and characterization of porous β-tricalcium phosphate blocks. Biomaterials 26:6099–6105.

Buck BE, Malinin TI. 1994. Human bone and tissue allografts. Preparation and safety. Clin Orthop Relat Res 303:8–17.

Burchardt H. 1983. The biology of bone graft repair. Clin Orthop Relat Res 174:28–42.

Cameron HU, MacNab I, Pilliar RM. 1977. Evaluation of a biodegradable ceramic. J Biomed Mater Res 11:179–186.

Cordell JM, Vogl ML, Wagoner Johnson AJ. 2009. The influence of micropore size on the mechanical properties of bulk hydroxyapatite and hydroxyapatite scaffolds. J Mechan Behavior Biomed Mater 2:560–570.

De Groot K. 1980. Bioceramics consisting of calcium phosphate salts. Biomaterials 1:47–50.

De Long WG, Einhorn TA, Koval K, McKee M, Smith W, Sanders W, Watson T. 2007. Bone grafts and bone graft substitutes in Orthopedic trauma. J Bone Joint Surg Am 89:649–658.

Dimitriou R, Mataliotakis GI, Angoules AG, Kanakaris NK, Giannoudis PV. 2011. Complications following autologous bone graft harvesting from the iliac crest and using RIA: A systematic review. Injury 42:3–15.

Donath K. 1988. Der Einbau von Knochenersatzmaterialien im Kieferknochen. Dtsch Zahnärztl Z 43:16–21.

Draenert K, Draenert Y. 1980. The vascular system of bone marrow. Scan Electron Microsc 4:113–122.

Draenert K, Draenert Y, Springorum HW, Gauer G, Müller ME, Willenegger HW. 1981. Histo-Morphologie des Spongiosadefektes und die Heilung des autologen Spongiosa-transplantates. In: 17. Jahrestagung der Deutschen Gesellschaft für Plastische und Wiederherstellungschirurgie. Cotta H, Martini AK, editors. Implantate und transplantate in der plastischen und wiederherstellungschirurgie. Berlin: Springer. pp. 88–92.

Draenert K, Wiese FG, Garde U, Draenert Y, Helber U, Börner M. 2001. Synthetische Knochenersatzwerkstoffe auf HA und TCP Basis. Trauma Berufskrankh 3:293–300.

Draenert K, Draenert M, Erler M, Draenert A, Draenert Y. 2011. How bone forms in large cancellous defects: Critical analysis based on experimental work and literature Injury. Int J Care Injured 42:47–55.

Draenert ME, Draenert AI, Forriol F, Erler M, Kunzelmann KH, Hickel R. 2012a. Value and limits of μ-CT for non-demineralized bone tissue processing. Anexperimental study to validate a standardized procedure. Microsc Res Tech 75:416–424.

Draenert K, Draenert Y, Pohlemann T, Regel G. 2012b. Autologous resurfacing and fracture dowelling. Heidelberg: Springer. pp. 41–52.

Dudley HR, Spiro D. 1961. The fine structure of bone cells. J Biophys Biochem Cytol 11:627–649.

Eggli PS, Müller W, Schenk RK. 1988. Porous hydroxyapatite and tricalciumphosphate cylinders with two different pore size ranges implanted in the cancellousbone of rabbits. A comparative histomorphometric and histologic study of bonyingrowth and implant substitution. Clin Orthop Relat Res 232:127–138.

FDA. 2003. Food and drug administration. Guidance for industry and FDA staff. Class II, spezial controlled guidance document: Resorbable calcium salt bone void filler device. Washington: CDRH.

Ferraro JW. 1979. Experimental evaluation of ceramic calcium phosphate as a substitute for bone grafts. Plast Reconstr Surg 63:634–640.

Fujita R, Yokoyama A, Nodasaka Y, Kohgo T, Kawasaki T. 2003. Ultrastructure of ceramic-bone interface using hydroxyapatite and beta-tricalcium phosphate ceramics and replacement mechanism of beta-tricalcium phosphate in bone. Tissue Cell 35:427–440.

Gerngross H, Burri C, Kinzl L, Merk J, Müller GW. 1982. Komplikationen an der entnahmestelle autologer spongiosatransplantate. Aktuelle Traumatol 12:146–152.

Gmelin L. 1957. Gmelins handbuch der anorganischen chemie. Weinheim: Verlag Chemie GmbH.

Holmes RE. 1979. Bone regeneration within a coralline hydroxyapatite implant. Plast Reconstr Surg 63:626.

Holmes RE, Mooney V, Bucholz R, Tencer A. 1984. A coralline hydroxyapatite bone graft substitute. Clin Orthop Relat Res 188:252–262.

Hoogendoorn HA, Renooij W, Akkermans LMA, Visser W, Wittebol P. 1984 Long-term study of large ceramic implants (porous hydroxyapatite) in dog femora. Clin Orthop 187:281.

Jarcho M. 1981. Calcium phosphate ceramics as hard tissue prosthetics. Clin Orthop Relat Res 157:259–278.

Jarcho M, Kay JF, Gumaer KI, Doremus RH, Drobeck HP. 1977. Tissue, cellular and subcellular events at a bone-ceramic hydroxyapatite interface. J Bioeng 1:79–92.

Klawitter JJ, Hulbert SF. 1971. Application of porous ceramics for the attachment of load bearing orthopedic applications. J Biomed Mater Res 17:769–784.

Klawitter JJ, Bagwell JG, Weinstein AM, Sauer BW, Pruitt JR. 1976. An evaluation of bone growth into porous high density polyethylene. J Biomed Mater Res 10:311–320.

Klein CP, Driessen AA, de Groot K, van den Hooff A. 1983. Biodegradation behavior of various calcium phosphate materials in bone tissue. J Biomed Mater Res 17:769–784.

Klinge B, Alberius P, Isaksson S, Jönsson J. 1992. Osseous response to implanted natural bone mineral and synthetic hydroxyapatite ceramic in the repair of experimental skull bone defects. J Oral Maxillofac Surg 50:241–249.

Koerten HK, van der Meulen J. 1999. Degradation of calcium phosphate ceramics. J Biomed Mater Res 44:78–86.

Kühne JH, Barti R, Frisch B, Hammer C, Jansson V, Zimmer M. 1994. Bone formation in coralline hydroxyapatite: Effects of pore sized studies in rabbits. Acta Orthop Scand 65:246–252.

Levin PM, Getter L, Cutright DE, Bhaskar SN. 1974. Biodegradable ceramic in periodontal defects. Oral Surg Med Oral Pathol 38:344–351.

Matti H. 1929. Über modellierende osteotomie und spongiosatransplantation. Schweiz Med Wochenschr 49:1254.

Matti H. 1932. Über freie transplantation von knochenspongiosa. Langenbecks Arch klin Chir 168:236.

Matti H. 1936. Technik und resultate meiner pseudarthrosenoperationen. Zbl Chir 63:1442–1451.

Meiss L. 1986. Untersuchung der knochenregeneration in standartisierten knochendefekten des göttinger miniaturschweins nach auffüllung mit zerkleinerten corticalis und porösen ca-phosphat keramiken. Habilitationsschrift der Medizinischen Fakultät. Hamburg.

Moore DC, Chapman MW, Manske D. 1987. The evaluationof a biphasic calcium phosphate ceramic for use in grafting long-bone diaphyseal defects. J Orthop Res 5:356–365.

Müller ME, Allgöwer M, Willenegger H. 1969. Manual der Ostheosynthese. Berlin: Springer.

Nade S, Armstrong L, Mc Cartney ER, Baggaley B. 1983. Osteogenesis after bone and bone marrow transplantation: The ability of ceramic materials to sustain osteogenesis from transplanted bone marrow cells. Preliminary studies. Clin Orthop Relat Res 181:217–225.

Ng AM, Tan KK, Phang MY, Aziyati O, Tan GH, Isa MR, Aminuddin BS, Naseem M, Fauziah O, Ruszymah BH. 2008. Differential osteogenetic activity of osteoprgenitor cells on HA and TCP/HA scaffold of tissue engineered bone. J Biomed Mater Res A 85:301–312.

Peelen JGJ, Rejda BV, Vermeiden JP, De Groot K. 1979. Sintered tricalcium phosphate as bioceramic. Ceramics 9:226.

Rahn BA, Perren SM. 1975. Die mehrfarbige fluoreszenzmarkierung desknochenbaus. Chem Rdsch 28:12–16.

Renooij W, Hoogendoorn HA, Visser WJ, Lentferink RHF, Schmitz MGJ, van Ieperen H, Oldenburg SJ, Janssen WM, Akkermans LMA, Wittebol P. 1985. Bioresorption of ceramic strontium-85-labeled calcium phosphate implants in dog femora. A pilot study to quantitate bioresorption of ceramic implants of hydroxyapatite and tricalcium orthophosphate in vivo. Clin Orthop Relat Res 197:272–285.

Robinson RA, Watson ML. 1952. Collagene-crystal-relationship in bone as seen in the electron microscope. Anat Rec 114:383–410.

Robinson RA, Watson ML. 1955. Crystal-collagene-relationship in bone as observed in the electron microscope. III. Crystal and collagene morphology as a function of age. Ann N Y Acad Sci 60:596–628.

Saxer U, Magerl F. 1974. Komplikationen nach spanentnahme aus dem beckenkamm. Helv Chir Acta 41:251–255.

Schenk R. 1974. Ultrastruktur des knochens. Verh Dtsch Ges Path 58:72–83.

Schieker M, Heiss C, Mutschler W. 2008. Bone substitutes. Unfallchirurg 111:613–620.

Schilling AF, Linhart W, Filke S, Gebauer M, Schinke T, Rueger JM, Amling, M. 2004. Resorbability of bone substitute biomaterials by human osteoclasts. Biomaterials 25:3963–3972.

Scott BL, Pease DC. 1956. Electron microscopy of the epiphyseal apparatus. Anat Rec 126:465–495.

Shimazaki K, Mooney V. 1985. Comparative study of porous hydroxyapatite and tricalcium phosphate as bone substitute. J Orthop Res 3:301.

Tadic D, Epple M. 2004. A thorough physicochemical characterization of 14 calcium phosphate-based bone substitution materials in comparison to natural bone. Biomaterials 25:987–994.

Tröster SD. 1993. Die hydroxylapatitkeramik endobon—eine alternative therapiemöglichkeit für knochendefekte. In: Venbrooks R, editor. Jahrbuch der Orthopädie. Zülpich: Biermann.

Uchida A, Nade SML, McCartney ER, Ching W. 1984. The use of ceramics for bone replacement. Clin Orthop Relat Res 66:269–275.

Urban RM, Turne TM, Hall DJ, Inoue N, Gitelis S. 2007. Increased bone formation using calcium sulfate-calcium phosphate composite graft. Clin Orthop Relat Res 459:110–117.

Vallet-Regi M. 2006. Revisiting ceramics for medical applications. Dalton Trans 28:5211–5220.

Weidenreich F. 1922. Über die beziehung zwischen muskelapparat und knochen und dem charakter des knochengewebes. Anat Anz 55:28–53.

Weidenreich F. 1923. Über aufbau und entwicklung des knochens und den charakter des knochengewebes. Z Anat 69:382–466.

Weidenreich F. 1930. Das Knochengewebe. In: Möllendorff V, editor. Handbuch der mikros-kopischen anatomie des menschen II Bd, 2. Teil. Berlin: Springer. pp. 390–520.

Wenisch S, Stahl JP, Horas U, Heiss C, Kilian O, Trinkaus K, Hild A, Schnettler R. 2003. In vivo mechanisms of hydroxyapatite ceramic degradation by osteoclasts: Fine structural microscopy. J Biomed Mater Res 67:713–718.

White RA, Weber JN, White EW. 1972. Replamineform: A new process forpreparing porous ceramic, metal, and polymer prosthetic materials. Science 176:922–924.

White E, Shors EC. 1986. Biomaterial aspects of Interpore-200 poroushydroxyapatite. Dent Clin North Am 30:49–67.

Wiese FG. 1998. Histomorphologie einer synthetisch hergestellten hydroxyl-apatit($Ca_5(PO_4)_3OH$) positivkeramik. Knochenersatzwerkstoff mit reproduzierbarer definierter Porengrösse im interkonnektierenden Porensystem. Dissertation Ludwig-Maximilians-Universität, München.

Winter MP, De Groot K, Tagar H, Heimke G, von Dijk HJA, Sawai K. 1981. Comparative histocompatibility testing of seven calcium phosphate ceramics. Biomaterials 2:159–162.

Wolff J. 1870. Über die innere architektur der knochenund ihre bedeutung für die frage von knochenzuwachs. Virchow Arch 50:389–450.

Yamada S, Heymann D, Bouler JM, Daculsi G. 1997. Osteoclastic resorption of calcium phosphate ceramics with different hydroxyapatite/beta-tricalcium phosphate ratios. Biomaterials 18:1037–1041.

Younger EM, Chapman MW. 1989. Morbidity at bone graft donor sites. J Orthopedic Trauma 3:192–195.